Predictive Modeling of Microcracking in Carbon-Fiber/Epoxy Composites at Cryogenic Temperatures

John F. Timmerman, James C. Seferis

Polymeric Composites Laboratory, Department of Chemical Engineering, University of Washington, Seattle, Washington 98195

Received 26 February 2003; accepted 28 May 2003

ABSTRACT: The temperature at which microcracking occurred in symmetrical cross-ply carbon-fiber/epoxy composite materials was predicted with a yield-stress-based failure model. A fracture mechanics analysis of the *in situ* strength of the ply groups in a composite material was combined with a compound beam determination of thermal stress development to create the predictive model. This approach, unlike many other models, incorporated the change in the material properties with temperature with the room-temperature properties of the laminate to predict the low-temperature behavior of the ply groups. Dynamic mechanical analysis was used to assess microcracking at cryogenic temperatures through the observation of discontinuities in the material properties during failure. Four different material systems were studied, and the model accurately predicted the onset temperature for microcracking in three of the four cases. It was shown that the room-temperature properties of a fiber-reinforced polymeric composite laminate, appropriately modified to account for property variations at low temperatures, could be used to predict transverse microcracking as a response to thermal stresses at cryogenic temperatures. © 2003 Wiley Periodicals, Inc. J Appl Polym Sci 91: 1104–1110, 2004

Key words: modeling; composites; thermal properties

INTRODUCTION

Background

Applications in which performance is critical and weight should be kept to a minimum have driven the adoption of fiber-reinforced polymeric composites over traditional monolithic structures. These materials achieve performance benefits through the combination of stiff, strong reinforcing fibers and a tough polymeric matrix that serves to protect and maintain the position of the fibers.[1] The resulting material is anisotropic, heterogeneous, and viscoelastic, and this creates the exceptional characteristics of fiber-reinforced composites but also introduces increasing levels of complexity and cost.[1–3]

Carbon-fiber/epoxy composite materials are anisotropic, and as the temperature of a composite material is lowered from its stress-free temperature, which is generally slightly higher than the cure temperature, thermal stresses are generated.[1] The composite laminate is composed of discrete parts, the epoxy matrix and the carbon fibers, that experience different dimensional changes as their temperature is altered. The carbon fibers contract in the radial direction and expand in the longitudinal direction when exposed to a decrease in temperature, whereas the epoxy matrix contracts in all directions as the temperature is reduced. This disparity causes thermal stresses to develop at the interface between the fibers and the matrix and also between the different ply groups in a composite laminate.[4–8] As the temperature becomes more removed from the cure temperature, these stresses increase. When they reach the yield stress of the material, microscale or macroscale failure results. For a cross-ply laminate, shown schematically in Figure 1, at a temperature below the stress-free temperature, the inner ply group is placed in a state of tension in the y direction and in a state of compression in the z direction. The outer ply groups experience the opposite situation, with compression in the y direction and tension in the z direction.[9] Initial failure occurs as a result of the generation of transverse tensile stresses because the ply groups are weakest in the transverse direction.[1]

Cryogenic liquid storage is an emerging application for carbon-fiber/epoxy composite structures. The thermal stresses that are present in these structures at subambient temperatures can cause fiber–matrix debonding, which leads to microscopic cracks that can propagate and eventually cause catastrophic fail-

Correspondence to: J. C. Seferis (seferis@cheme.washington.edu).

Contract grant sponsor: Air Force Office of Scientific Research; contract grant number: F49620-00-1-0132.

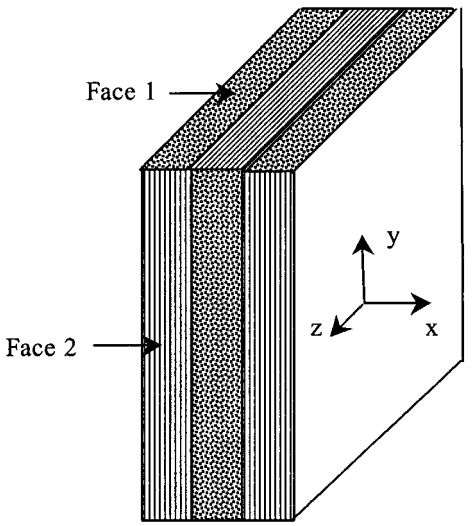

Figure 1 Schematic of cross-ply laminate.

ure.[10–17] The failure of composite materials exposed to thermal cycling and thermal stresses is a serious concern. Because of this, many attempts have been made to predict the generation of thermal stresses in composite materials, the onset of microcracking, and the distribution and origination of microcracks during failure. Shear lag analyses, variational and strain energy release rate approaches, Monte Carlo simulations, and *in situ* strength analyses are among the approaches that have been used to address this problem.[8,18–22] Various degrees of success have been achieved with these analyses, but they are often unnecessarily complex and fail to account for the changes in the material properties with temperature. The strength and modulus of the laminate and its components, particularly the viscoelastic polymeric matrix, are altered when they are exposed to significant decreases in temperature; this results in stress generation and failure criteria that are different from those at room temperature.[1,10,23–26]

In this study, the onset temperature for microcracking in symmetrical cross-ply carbon-fiber/epoxy laminates was predicted with a straightforward stress-based failure model. The model incorporated fracture mechanics and the variation in the laminate properties as the temperature was decreased so that a few simple room-temperature experiments could be used to describe failure from thermal stresses at low temperatures.

Model development

Brand and Backer[27] developed a compound beam analysis that could be adapted to describe the generation of thermal stresses in laminated materials. The advantage of this approach is that it takes into account stress relaxation during curing and cooling. The foundation of the compound beam analysis involves considering the ply groups as individual elastic entities and calculating the stresses that result from thermal expansion and contraction.[6,27] The transverse tensile thermal stress in the central plies of a symmetrical cross-ply laminate (σ_{tl}^{th}) was derived with compound beam theory and can be described by the following equation. Equation (1) was modified to account for the changes in the material properties with temperature:

$$\sigma_{tl}^{th} = \frac{-E_t(T)E_l(T)\int_{T_{SFT}}^{T_{Use}}[[\alpha_t(T) - \alpha_l(T)]\,dT]}{E_l(T) + E_t(T)} \quad (1)$$

where T_{Use} is the use temperature of the laminate [or average onset temperature for microcracking (°C)]; T_{SFT} is the stress-free temperature (°C); E_l and E_t are the longitudinal and transverse moduli (Pa), respectively, of a unidirectional laminate with the same thickness as the ply group expressed as a function of temperature; and α_l and α_t are the longitudinal and transverse linear coefficients of thermal expansion ($°C^{-1}$), respectively. It is proposed that microcracking will occur at the temperature that sets the thermal transverse tensile stress in the central ply group equal to the *in situ* yield strength. Past work by Wang and Karihaloo[20] and Laws and Dvorak[28] showed that the yield strength of this ply group (Y_t) could be expressed as follows:

$$Y_t = \frac{\sqrt{G_{IC}(T)E_t(T)}}{F_I\sqrt{a}} \quad (2)$$

The original expression has been modified to account for the variation in the material properties with temperature. G_{IC} is the critical strain energy release rate (N/m), E_t is the transverse modulus of the ply group in a plane-stress condition, F_I is a factor derived from fracture mechanics, and a is the initial half-crack length (m). The $F_I(a)^{1/2}$ term can be expressed as a constant [C ($m^{1/2}$)]. The following expression was produced from a combination of eqs. (1) and (2) and can be solved to obtain the temperature at which failure will first occur:

$$\frac{\sqrt{G_{IC}(T)E_t(T)}}{C} = \frac{-E_t(T)E_l(T)\int_{T_{SFT}}^{T_{Use}}[[\alpha_t(T) - \alpha_l(T)]\,dT]}{E_l(T) + E_t(T)} \quad (3)$$

A model laminate system was developed to determine C and describe the temperature dependence of the material properties. The thermal stress in the laminate

TABLE I
Prepeg Characteristics

Prepreg	Carbon fiber	Epoxy formulation	Curing agent	Prepreg resin content (wt %)	Prepreg fiber areal weight (g/m^2)
1	T300 YC	3:1 1031:828	DDS	54.7 (0.77)	124.0 (2.26)
2	T300 YC	3:2 1031:828	DDS	45.3 (0.65)	129.9 (1.60)
3	T300 YC	2.4:2:1 828:661:1031	DICY/diuron	47.0 (1.00)	144.5 (2.40)
4	T-50S	—	—	47.7 (0.021)	100.0

at the first failure event was calculated from the observed material parameters and the experimentally determined microcracking onset temperature. The thermal stress at failure was then set equal to the yield stress, and eq. (3) was solved to determine *C*. This value of *C* was used in the model predictions for all the subsequent materials.

EXPERIMENTAL

Material development

Four different unidirectional, prepreg-based carbon-fiber/epoxy composite systems were used to determine the model parameters and validate its effectiveness. Three of these prepregs (denoted prepregs 1–3) were prepared in the laboratory, and one (prepreg 4) was supplied from an outside industrial source. The industrial material was used to assess the performance of the model in relation to a material with a less well-known composition and processing history. The four prepregs are outlined in Table I. The numbers in parentheses indicate standard deviations.

A mixture of commercially available epoxy resins formed the base of the polymeric matrix for the prepregs prepared in the laboratory. The resins used were EPON 828 and 1031 from Resolution Performance Products and DER 661 from Dow Chemical Co. EPON 828 and DER 661 are based on diglycidyl ether of bisphenol A and have different backbone lengths. EPON 828 has an epoxy equivalent weight (EEW) of 187 g/epoxy, and DER 661 has an EEW of 530 g/epoxy. EPON 1031 is a tetrafunctional aromatic epoxy resin. Diaminodiphenyl sulfone (DDS; HT 976, Ciba) and dicyandiamide (DICY; Amicure CG 1400, Pacific Anchor Chemical Co.), accelerated with diuron from Aldrich Chemical Co., were used as the curing agents.

The epoxy resins were combined in the weight ratios shown in Table I in an oil bath at 120°C and stirred until they were completely mixed. For prepreg systems 1 and 2, a stoichiometric amount of DDS was melted and added to the epoxy mixture in the oil bath. The epoxy/DDS mixture was blended for 2 min in the oil bath at 120°C, after which the resin was cooled to 80°C and prepregged. For prepreg system 3, half of 828 was set aside and blended with 5 phr (parts per hundred parts of resin) DICY and 2 phr diuron in a high-shear mixer to form a curing paste. The epoxy mixture was blended and allowed to cool to 80°C, at which point the curing paste was added. After the paste was blended with the epoxies, the mixture was prepregged.

Unidirectional prepregs were developed consisting of the aforementioned resins and epoxy-sized Toray 50C T300YC carbon fibers. The filament count for all of the fibers was 12,000 per tow. A hot-melt prepreg machine was used to impregnate the fibers with the epoxy resin.[29] The prepreg fiber areal weight and the nominal resin content for the different prepregs are shown in Table I. The filming and impregnation temperatures were 82 and 93°C, respectively. Two rollers were used to apply the impregnation pressure. The pressure on the first roller was 69 kPa, and the pressure on the second was 138 kPa. The line speed was 1.5 m/min, and the gap height for resin filming was 0.30 mm.

Weighing a 5.08 cm × 5.08 cm square of a prepreg, dissolving the resin with acetone, and weighing the dried fibers determined the resin content of a prepreg. This technique agreed with ASTM D 3171-99 and Boeing Support Standard 7336.[30,31] Five samples from each prepreg batch were used to measure the resin content.

Symmetrical, unsymmetrical, and unidirectional 10.16 cm × 10.16 cm laminates and unidirectional 33.02 cm × 12.7 cm laminates were laid up with the aforementioned prepregs. The symmetrical laminates consisted of 12 plies of a prepreg in a $[0^o_3, 90^o_3]_S$ configuration. The unsymmetrical laminates consisted of four plies in a $[0^o_2, 90^o_2]$ configuration. The 10.16 cm × 10.16 cm unidirectional laminates consisted of 6 plies, and the 33.02 cm × 12.7 cm unidirectional laminates consisted of 16 plies with a 5.08-cm fluorinated ethylene–propylene copolymer crack starter placed in the midplane.

The aforementioned laminates were exposed to an autoclave cure cycle that consisted of a 2.77°C/min ramp to 93°C, a 1-h hold at 93°C, a ramp at 2.77°C/min to 177°C, a 2-h hold at 177°C, and a ramp to 25°C at 2.77°C/min. The total consolidation pressure used during the cure was 310 kPa. The vacuum bag was vented to the atmosphere when the autoclave pressure reached 104 kPa.

Once cured, the symmetrical laminates were cut with a diamond saw into 3.49 cm × 1.27 cm (length × width) samples for cycling studies, and the 6-ply unidirectional laminates were cut into 5.08 cm × 1.27 cm (length × width) transverse and longitudinal samples for modulus determination. The unsymmetrical laminates were cut into 20.0 cm × 1.27 cm (length × width) samples for the determination of the stress-free temperature, and the 16-ply unidirectional laminates were cut into 33.02 cm × 1.27 cm (length × width) samples for fracture toughness testing. The edges of the cycling and modulus samples were polished before testing to facilitate optical microscopy of the surfaces.

Testing and analysis

Mode I interlaminar fracture toughness (G_{IC}) was measured with the double-cantilever beam method.[32] For each laminate, five samples were tested. Each sample was precracked before testing to create a sharp crack tip. The specimens were pulled apart at a rate of 25.4 mm/min with an Instron 4505 screw-testing frame controlled by Instron Series IX software.

The longitudinal and transverse tensile moduli of the 6-ply unidirectional samples were determined with a Seiko SII 6100 dynamic mechanical spectrometer controlled by Exstar 6000 (version 6.0). The samples were exposed to a 2.5 N load for 10 s and then held at a zero load for 10 s. This process was repeated as the samples were heated at 5°C/min from −120 to 170°C. From the resulting position and load data, modified to account for thermally induced dimension changes in the samples, the modulus during each loading cycle could be determined. The dependence of the modulus on the temperature was quantified with these data. The samples were examined with optical microscopy before and after testing to ensure that no cracks or failure sites were formed during testing.

Dynamic mechanical analysis (DMA) experiments were performed on the cured unsymmetrical laminates in a controlled-force three-point-bending mode with a TA Instruments 2980 DMA instrument controlled by Thermal Solutions 1.2 J software. The samples were exposed to a 2°C/min ramp to 250°C with an applied force of 0.005 N. The stress-free temperature of each sample was reported as the temperature at which each laminate displayed zero curvature.[9,33]

The unidirectional samples from the G_{IC} tests were used to fabricate 1.0 cm × 1.0 cm samples for the determination of the longitudinal and transverse coefficients of thermal expansion of the laminates. Each sample was obtained from a portion of the fracture toughness specimen that was not damaged during testing. The coefficient of thermal expansion was determined with a TA Instruments 2940 thermomechanical analyzer controlled by Thermal Solutions 1.2 J software. A heating rate of 5°C/min from −100 to 170°C was used with a macroexpansion probe and a force of 0.05 N in nitrogen. The dependence of the coefficient of thermal expansion on the temperature was determined from the slope of the dimension change between −100 and 170°C. This technique was performed according to ASTM E 831-93.[34]

The cut and polished symmetrical laminates were allowed to equilibrate at 22°C and were then cooled to a specified temperature and held for 10 min in the 6100 dynamic mechanical spectrometer described earlier. The microcracking onset temperature was determined by the lowering of the hold temperature in 5°C increments between runs until microcrack formation was observed. During cycling, the laminates were deformed at a frequency of 1 Hz with an oscillation amplitude of 10 μm to identify changes in the dynamic mechanical behavior at low temperatures and as microcracking occurred. Previous experiments showed that deformation of this type and duration did not change the microcracking behavior of these samples.

Optical microscopy was used to observe and document the response of the samples to cryogenic exposure. Five samples from each laminate were tested to determine the onset temperature for microcracking. Each sample was examined before it cooled to ensure that there were no initial cracks or defects on the surface. After each material had returned to room temperature, it was examined at 50, 100, and 200× magnifications with an optical microscope. Photomicrographs were taken to document the sample response, and the size and morphology of the microcracks on the polished surface were recorded.

RESULTS AND DISCUSSION

Microcracking

DMA of the symmetrical laminates at cryogenic temperatures revealed information about the low-temperature properties of composite materials and the effects of microcracking on their response to dynamic loads. The storage modulus (E') and tan δ during exposure to subambient temperatures are shown in Figure 2 for a symmetrical cross-ply laminate made from prepreg 2. Figure 2(A) demonstrates that E' of the laminate increased as the temperature decreased, establishing that the properties of the laminates studied changed significantly at low temperatures. Therefore, the temperature dependence of the material properties must be explained in a predictive model of microcracking at cryogenic temperatures.

The sharp, discontinuous decrease in E' shown in Figure 2(A) and the spike in tan δ shown in Figure 2(B) corresponded to the onset of microcracking in the laminate. An examination of the laminate after cycling

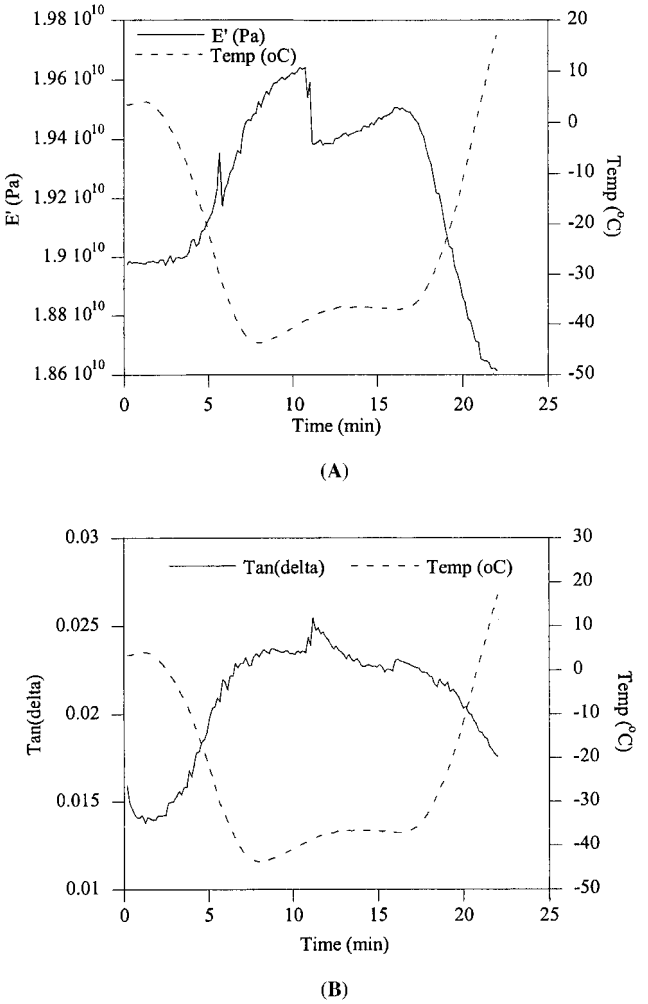

Figure 2 Effects of cryogenic temperatures and microcracking on the dynamic mechanical properties of symmetrical laminates: (A) E' and (B) tan δ.

revealed the formation of a microcrack spanning the interior ply group of face 2 of the laminate, as defined in Figure 1. A similar E' and tan δ response appeared in all of the laminates in which microcracking was observed. Microcrack formation reduced the stiffness of the laminate and caused a momentary increase in the phase lag. Microcracking debonded the fibers from the matrix and prevented efficient load transfer, reducing the modulus of the sample, increasing the ability of the laminate to dissipate energy at the fiber–matrix interface, and causing an increase in tan δ.[35,36]

Microcracking was observed in the laminates made from prepregs 1, 2, and 4 as a response to cryogenic cycling. The majority of the microcracks spread across the entire width of the central plies in face 2 and propagated through the laminate. When the microcracks reached the interface between the 0 and 90° ply groups, delamination was observed in some cases. Figure 3 presents optical photomicrographs of representative microcracks formed during cryogenic cycling. Figure 3(A) shows the microcrack formed during the thermal cycle in Figure 2. Figure 3(B,C) illustrates the formation and extension of a small crack during exposure to progressively lower temperatures. In some cases, as shown in Figure 3(A), microcracks formed effectively instantaneously and propagated through the sample; at other times, as demonstrated in Figure 3(B,C), small cracks formed initially and gradually extended through the sample.

The microcracks propagated along the fiber–matrix interface and demonstrated considerable variation in width and morphology. Irregularities in crack size and shape introduced significant error into the prediction of the number and distribution of microcracks as one large, tortuous crack may have dissipated as much energy as the formation of two smaller cracks. It is for this reason that the objective of this study was to predict the onset of microcracking and not the specific number or distribution of failure events.

Model predictions

The important material properties, specifically the coefficients of thermal expansion and the longitudinal and transverse tensile moduli, varied with temperature to different extents, ranging from being effectively constant to depending strongly on the temperature. The linear and transverse coefficients of thermal expansion did not exhibit temperature dependence

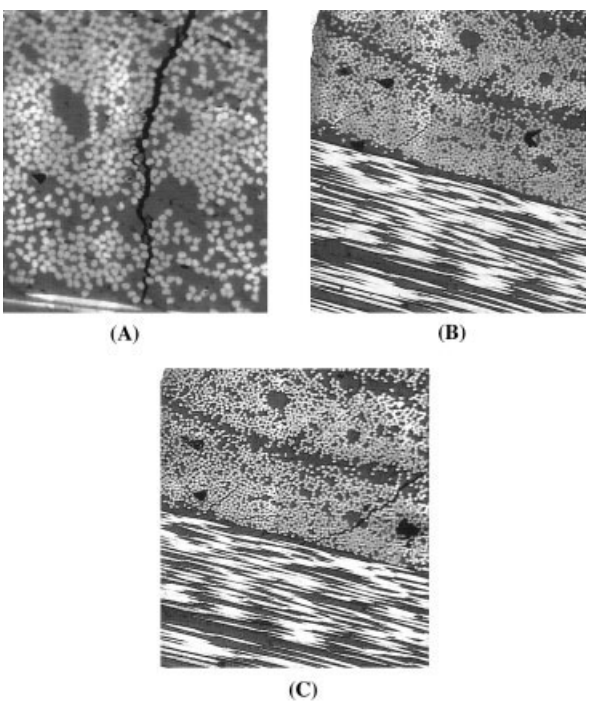

Figure 3 Optical photomicrographs of microcracks: (A) prepreg 2 (200×, −40°C), (B) prepreg 1 (100×, −40°C), and (C) prepreg 1 (100×, −60°C; an extension of the crack from part B).

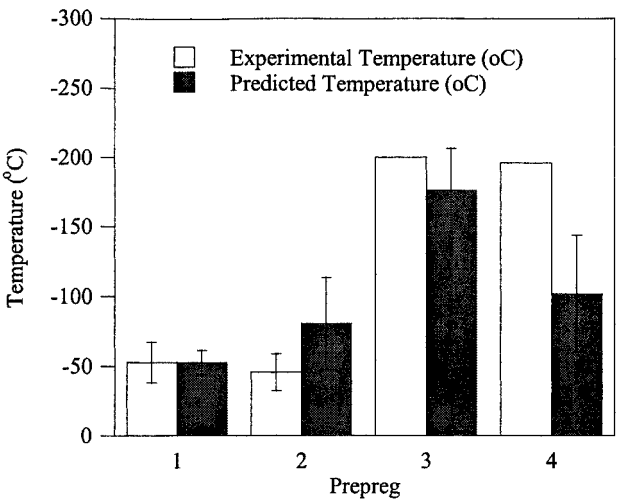

Figure 4 Comparison of predicted and experimental microcracking onset temperatures.

between −100 and 170°C for the carbon-fiber/epoxy laminates studied. The longitudinal tensile modulus showed a small linear increase with decreasing temperature, with a typical increase of 0.08% after cooling from 25 to −120°C. The transverse tensile modulus, which played a key role in the development of transverse tensile stresses, showed a significant linear increase with decreasing temperature, increasing on average 25% from 25 to −120°C. G_{IC} as a function of temperature was unknown and was unable to be determined; therefore, an additional factor accounting for changes in the fracture behavior at low temperatures was grouped into constant C in eq. (3).

T_{Use}, T_{SFT}, $E_l(T)$, $E_t(T)$, $\alpha_l(T)$, $\alpha_t(T)$, and G_{IC} for the laminates made from prepreg 1 were used to solve eq. (3) for C. C was calculated to be 0.036 ± 0.0062 $m^{1/2}$. Once C was determined, the model could be applied to other material systems.

Figure 4 illustrates the effectiveness of the model in predicting the microcracking onset temperature, with the error bars indicating one standard deviation. The error bars are relatively large because of the variation in the microcrack size and shape between each failure event. Error bars are not present at the observed microcracking temperature for prepregs 3 and 4 because fewer than three of five samples formed microcracks and a standard deviation could not be calculated. The microcracking temperatures were essentially the same for prepregs 1 and 2, and this was consistent with their similar compositions. The use of DICY/diuron as the curing agent in prepreg 3 increased the microcracking temperature, and this was consistent with past results.[37] The model correctly predicted the onset of microcracking for laminates made from prepregs 1–3. In the case of prepreg 4, the model predicted microcracking between −140 and −60°C, whereas microcracking actually occurred at −190°C.

The microcracking temperature may have been underpredicted for prepreg 4 because it was supplied by an industrial source. The properties of this material were less accurately known than those of the prepregs that were produced in the laboratory. It was also possible that the longitudinal and transverse coefficients of thermal expansion were no longer temperature-independent or that the dependence of the tensile moduli on temperature deviated from linearity as the temperature approached the microcracking temperature (≈−200°C). Instrumental limitations prevented the recording of data below −120°C; therefore, the property variation with temperature trends in the −100 to 0°C temperature range were extended to lower temperatures.

CONCLUSIONS

Symmetrical, cross-ply carbon-fiber/epoxy laminates were produced and exposed to subambient temperatures to determine the microcracking onset temperature. These data were then compared with the predictions of a stress-based compound beam model in which fracture mechanics was used to determine the *in situ* yield strength of the ply groups in the laminates, and the variation in the material properties at low temperatures was explained. The model correctly predicted the failure temperature for most of the materials tested. In addition, it showed that accurate predictions of thermal-stress-induced failure could be made with the room-temperature properties of a laminate, appropriately modified to account for low-temperature property variations. Microcracking changed the dynamic mechanical properties of the composite materials studied, and it was shown that DMA could be used to assess the formation of microcracks.

The authors thank the Air Force Office of Scientific Research for its project support of the Polymeric Composites Laboratory at the University of Washington.

References

1. Mallick, P. K. Fiber Reinforced Composites: Materials, Manufacturing, and Design, 2nd ed.; Marcel Dekker: New York, 1993.
2. Hoisington, M. Process/Property Interrelations of Layered Structured Composites; University of Washington: Seattle, WA, 1992.
3. Seferis, J. C.; Hillermeier, R. W.; Buehler, F. U. In Polymer Matrix Composites; Talreja, R.; Manson, J.-A. E., Eds.; Elsevier: Oxford, 2001.
4. Simpson, M.; Jacobs, P. M.; Jones, F. R. Composites 1991, 22, 89.
5. Spain, R. G. Composites 1971, 33.
6. Bailey, J. E.; Curtis, P. T.; Parvizi, A. Proc R Soc London Ser A 1979, 366, 599.
7. Brinkman, M. R.; Sarrazin, H. J Reinforced Plast Compos 1995, 14, 1252.
8. McManus, H. L.; Bowles, D. E.; Tompkins, S. S. J Reinforced Plast Compos 1996, 15, 124.
9. Crasto, A. S.; Kim, R. Y. J Reinforced Plast Compos 1993, 12, 545.

10. Wigley, D. A. Basic Cryogenics and Materials; NASA-CR-177932; NASA: 1985.
11. Toth, J. M., Jr.; Bailey, W. J.; Boyce, D. A. Fiberglass Epoxy Laminate Fatigue Properties at 300 and 20 K; 1985.
12. Toth, J. M.; Bailey, W. J.; Boyce, D. A. In ASTM STP 857; Stephens, R. I., Ed.; American Society for Testing and Materials: Philadelphia, 1985.
13. Ambur, D. R.; Sikora, J.; Maguire, J. F.; Winn, P. M. Development of a Pressure Box to Evaluate Reusable-Launch-Vehicle Cryogenic-Tank Panels; NASA-TM-11406; AIAA Paper 96-1640; NASA: 1996.
14. Nelson, K. M. Composites in Cryogenic Fuel Tank Applications; Boeing Materials Technology/Phantom Works: 1999.
15. Liokhman, V. V.; Kopsitskaya, L. N.; Muratov, V. M. Khim Neftyanoe Mashinostroenie 1997, 6, 22.
16. Nguyen, B. Proc Int SAMPE Conf 1999, 44, 856.
17. Wood, C.; Bradley, W. In Fiber Matrix and Interface Properties; ASTM STP 1290; Spragg, C. J.; Drzal, L. T., Eds.; American Society for Testing and Materials: Philadelphia, 1996.
18. Nairn, J. A. J Compos Mater 1989, 23, 1106.
19. Michii, Y.; McManus, H. L. J Reinforced Plast Compos 1997, 16, 1220.
20. Wang, J.; Karihaloo, B. L. J Compos Mater 1996, 30, 1314.
21. Wang, J.; Karihaloo, B. L. J Compos Mater 1996, 30, 1338.
22. Takeda, N.; Ogihara, S. Compos Sci Technol 1994, 52, 183.
23. Rodriguez, F. Principles of Polymer Systems, 4th ed.; Taylor & Francis: Washington, DC, 1996.
24. Markley, F. W.; Hoffman, J. A.; Muniz, D. P. Adv Cryog Eng 1986, 32, 119.
25. Schaffer, J. P.; Saxena, A.; Antolovich, S. D.; Sanders, T. H., Jr.; Warner, S. B. The Science and Design of Engineering Materials; Irwin: Chicago, 1995.
26. Nettles, A. T.; Biss, E. J. Low Temperature Mechanical Testing of Carbon-Fiber/Epoxy-Resin Composite Materials; NASA-TP-3663; NASA: 1996.
27. Brand, R. H.; Backer, S. Text Res J 1962, 32, 39.
28. Laws, N.; Dvorak, G. J. Int J Solids Struct 1987, 23, 1269.
29. Putnam, J. W.; Hayes, B. S.; Seferis, J. C. J Adv Mater 1996, 27, 47.
30. Standard Test Methods for Constituent Content of Composite Materials; ASTM D 3171-99; American Society for Testing and Materials: West Conshohocken, PA, 1999.
31. Resin Content and Fiber Areal Weight of Prepreg Fabric and Tape, Test Method for; BSS 7336; Boeing Materials Technology: Renton, WA, 1996.
32. Pagano, N. J. Interlaminar Response of Composite Materials; Elsevier: New York, 1989.
33. Pagano, N. J.; Hahn, H. T. Composite Materials: Testing and Design; ASTM STP 617; American Society for Testing and Materials: Philadelphia, 1977.
34. Standard Test Method for Linear Thermal Expansion of Solid Materials by Thermomechanical Analysis; ASTM E 831-93; American Society for Testing and Materials: West Conshohocken, PA, 1993.
35. Kennedy, J. M.; Edie, D. D.; Banerjee, A.; Cano, R. J. J Compos Mater 1992, 26, 869.
36. Adams, D. S.; Bowles, D. E.; Herakovich, C. T. J Reinforced Plast Compos 1986, 5, 152.
37. Timmerman, J. F.; Tillman, M. S.; Hayes, B. S.; Seferis, J. C. Compos A 2002, 33, 323.